Supramolecular Chemistry

DOI: 10.1002/ange.201001676

Highly Selective Ratiometric Emission Color Change by Zinc-Assisted Self-Assembly Processes**

Takuya Ogawa, Junpei Yuasa, and Tsuyoshi Kawai**

Switches are key elements in the construction of complex supramolecular systems and for their use as sensing molecules. In the case of fluorescence sensors, simple "off/on" switching based on host–guest interaction is the most popular use at present.[1–3] However, supramolecular systems involving multiple species can interconvert between two or more self-assembled units when these distinct states are on a relatively flat potential energy surface.[4–8] This strategy has opened ways to create unique sensing systems with nonlinear (e.g., "off/on/off" or "off/off/on") switching ability.[9–13] As a prototypical example, fluorescence probes comprised of multidentate ligands show nonlinear intensity changes[9,10] or ratiometric shifts[12,13] of emission upon sequential binding of metal ions. This method allows us to assess changes in the metal ion concentration by observing the threshold of nonlinear intensity changes[9–11] or ratiometric color changes in emission.[12,13] However, such systems that contain relatively simple binding motives often show similar fluorescence modulation to that obtained with the target metal ion, because ligands also bind with competing metal ions.[10]

We report herein a highly selective ratiometric emission color change of 2-(anthracen-9-ylethynyl)-1-methylbenzimidazole (BzIm-An) by well-defined self-assembly processes with Zn^{2+}.[14] Interconversion between two successive complex species of BzIm-An with Zn^{2+} enables the first observation of "off/on/off" switching of anthracene dimer emission (Scheme 1a).[15,16] This unique assembling feature of BzIm-An allows us to create new sensing mechanisms to enable fine-tuning of the emission color as a function of Zn^{2+} concentration.

The emission response of BzIm-An to $Zn(OTf)_2$ (OTf = OSO_2CF_3) over a wide concentration range is shown in Figure 1. We focused on Zn^{2+} in the first experiment because of its importance as an active ion in biological systems.[17] The original blue emission of BzIm-An is changed to light yellow in the presence of low concentrations of Zn^{2+} (3.6×10^{-5}–1.4×10^{-3} M), and in turn is subsequently changed to green in the high-concentration region ($>7.0\times10^{-3}$ M; inset of Figure 1). The CIE chromaticity diagram (CIE = International Commission on Illumination) for the emission of BzIm-An at various concentrations of Zn^{2+} demonstrates the fine-tuning of the emission color from blue to light yellow to green in response to Zn^{2+} concentration (Figure 1).

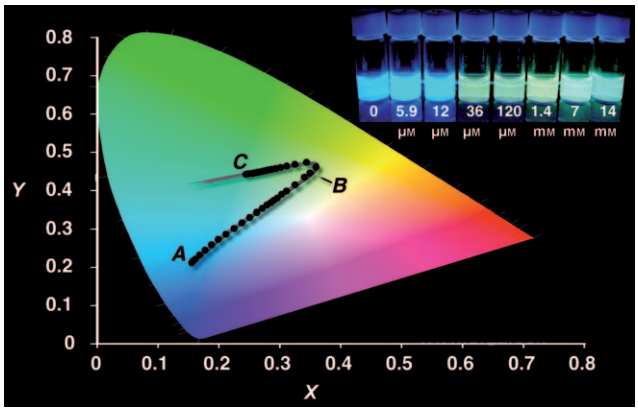

Figure 1. CIE chromaticity diagram for the emission of BzIm-An (5.0×10^{-5} M) in the presence of Zn^{2+} (A: 0 M to B: 7.5×10^{-5} M to C: 6.6×10^{-2} M) in MeCN at 298 K. Excitation wavelength $\lambda = 438$ nm. Inset: Photographs of solutions of BzIm-An (5.0×10^{-5} M) in the presence of Zn^{2+} (0–1.4×10^{-2} M) in MeCN under irradiation with UV light.

UV/Vis and fluorescence spectral titrations of BzIm-An by Zn^{2+} were performed to understand how BzIm-An allows multicolor tuning of emission as a function of Zn^{2+} concentration (see below). Upon addition of low concentrations of Zn^{2+} ($<7.5\times10^{-5}$ M) to a solution of BzIm-An in acetonitrile, UV/Vis spectral changes of BzIm-An were observed with isosbestic points at $\lambda = 438$, 346, 325, and 305 nm; the characteristic anthracene absorption at $\lambda = 408$ nm (Figure 2a, red line) was suppressed and a broad absorption band appeared at longer wavelengths (Figure 2a, yellow line). Similarly, the characteristic anthracene fluorescence band at $\lambda = 469$ nm (Figure 2b, red line) gradually changed to a broad structureless emission band (Figure 2b, yellow line) with increasing Zn^{2+} concentration, which is characteristic of the emission spectrum of anthracene dimers.[18,19] The stacking of anthracene moieties is ascribed to complex formation of BzIm-An with Zn^{2+}. Hence, the absorbance at $\lambda = 408$ nm and the emission intensity at $\lambda = 494$ nm were plotted against the ratio of Zn^{2+} concentration to the initial concentration of BzIm-An ($[Zn^{2+}]/[BzIm\text{-}An]_0$) to determine the stoichiometry of the Zn^{2+} complex (inset of Figure 2a, top and bottom panels, respectively).

[*] T. Ogawa, Dr. J. Yuasa, Prof. Dr. T. Kawai
Graduate School of Materials Science
Nara Institute of Science and Technology
8916-5 Takayama, Ikoma, Nara 630-0192 (Japan)
Fax: (+81) 743-72-6179
E-mail: yuasaj@ms.naist.jp
tkawai@ms.naist.jp
Homepage: http://mswebs.naist.jp/center/LABs/kawai/

[**] This work supported in part by a Grant-in-Aid for Scientific Research on Innovative Areas (Molecular Science of Fluctuations toward biological Functions).

Supporting information for this article is available on the WWW under http://dx.doi.org/10.1002/anie.201001676.

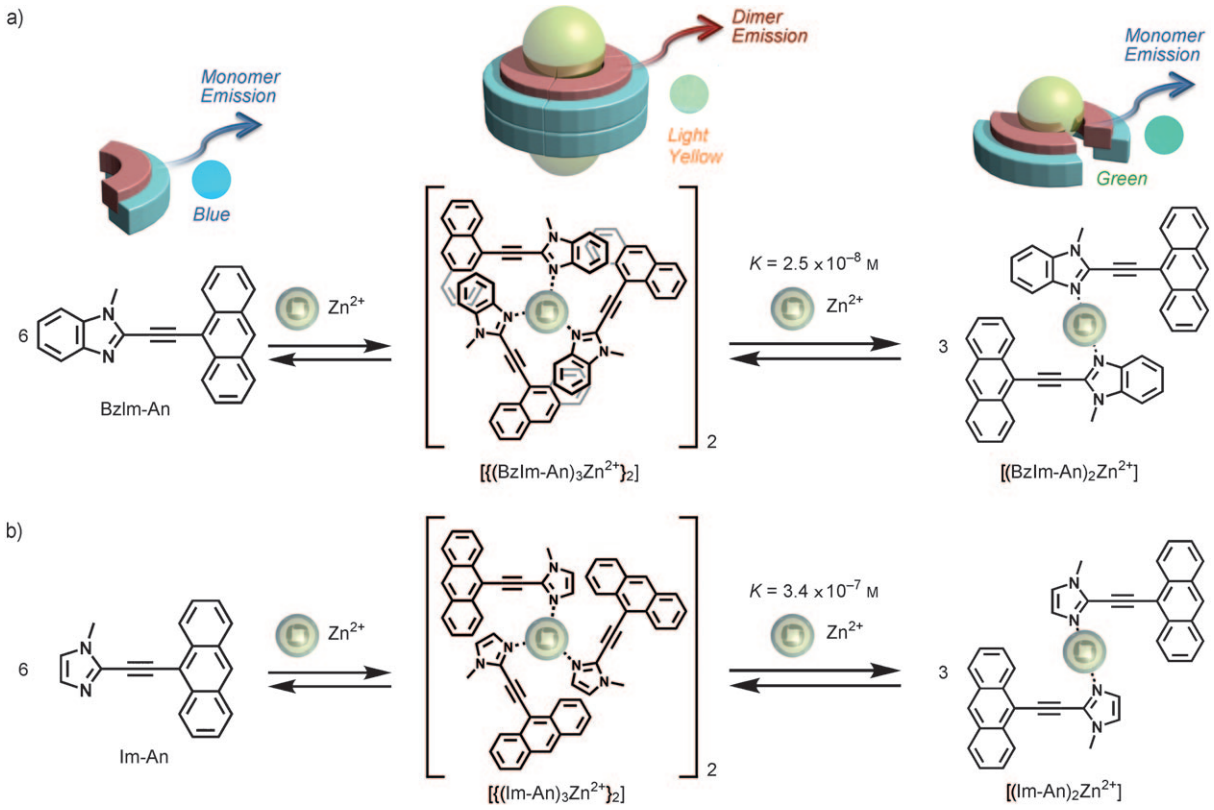

Scheme 1. Stepwise complex formation of Zn^{2+} with a) BzIm-An and b) Im-An. Note the visible emission color change of BzIm-An.

The titration curves reveal a stoichiometry of three BzIm-An ligands bound per Zn^{2+} ion ($[Zn^{2+}]/[BzIm\text{-}An] = 0.33$). However, all possible coordination geometries of a simple 3:1 complex $[(BzIm\text{-}An)_3Zn^{2+}]$ could not bring the two anthracene rings in a face-to-face position. Thus, π-stacked anthracene moieties may be ascribed to π-stacking between the 3:1 complexes ($[\{(BzIm\text{-}An)_3Zn^{2+}\}_2]$) [first step of Scheme 1 a], which was evidenced by ESI MS and NOE experiments (see below).

The broad emission band of $[\{(BzIm\text{-}An)_3Zn^{2+}\}_2]$ at $\lambda =$ 554 nm overlaps with the weak emission peaks at $\lambda = 444$ and 472 nm (Figure 2 b, yellow line). The excitation spectra recorded at $\lambda = 444$ and 554 nm [inset of Figure 2 b (top)] are close to the absorption spectra of free BzIm-An and $[\{(BzIm\text{-}An)_3Zn^{2+}\}_2]$, respectively (Figure 2 a, red and yellow lines, respectively), thereby indicating that the weak emission bands at the shorter wavelengths are due to the fluorescence of the small amount of BzIm-An generated in the dissociation equilibrium of $[\{(BzIm\text{-}An)_3Zn^{2+}\}_2]$ (leftward arrow in the first step of Scheme 1 a).

Time-resolved fluorescence measurements of BzIm-An in the presence of a low concentration of Zn^{2+} (6.0×10^{-4} M) confirm the ground-state dimerization of anthracene moieties (see below). Analysis of the excited-state dynamics immediately after laser irradiation (1.0 ns) of BzIm-An shows a broad emission band of $[\{(BzIm\text{-}An)_3Zn^{2+}\}_2]$ at $\lambda = 554$ nm overlapping with the weak fluorescence at $\lambda = 472$ nm due to the unbound BzIm-An [inset of Figure 2 b (bottom), green line]. These two components decay independently, and the fluorescence band due to free BzIm-An at a shorter wavelength totally disappears upon laser excitation within 14.4 ns [inset of Figure 2 b (bottom), yellow line]. The emission lifetimes of $[\{(BzIm\text{-}An)_3Zn^{2+}\}_2]$ were determined separately from biexponential emission decays (see the Supporting Information S1). The excited-state lifetime of $[\{(BzIm\text{-}An)_3Zn^{2+}\}_2]$ (23.9 ns) is much longer than that of free BzIm-An (4.0 ns), indicating anthracene dimer emission from $[\{(BzIm\text{-}An)_3Zn^{2+}\}_2]$.

However, the absorption and emission spectra of $[\{(BzIm\text{-}An)_3Zn^{2+}\}_2]$ show additional changes in the presence of large excess of Zn^{2+} ($> 1.5 \times 10^{-3}$ M) [Figure 2 a,b, blue lines], namely, the emission band of the anthracene dimer is replaced by a broad emission band at shorter wavelength (Figure 2 b, blue line). Such stepwise spectral changes are ascribed to the conversion of the $[\{(BzIm\text{-}An)_3Zn^{2+}\}_2]$ complex into another complex species that has no stacked anthracene moieties (second step of Scheme 1 a). A plot of the emission intensity at $\lambda = 494$ nm versus the concentration of Zn^{2+} clearly demonstrates the nonlinear "off/on/off" switchability of the emission of BzIm-An through stepwise complex formation (Figure 2 c): The emission intensity decreases with increasing Zn^{2+} concentration to approach the saturation value in the low-concentration region of Zn^{2+} ($< 1.5 \times 10^{-3}$ M), after which the emission intensity starts to increase with increasing Zn^{2+} concentration. The saturated dependence of the emission intensity on $[Zn^{2+}]$ at the high-concentration region of Zn^{2+}

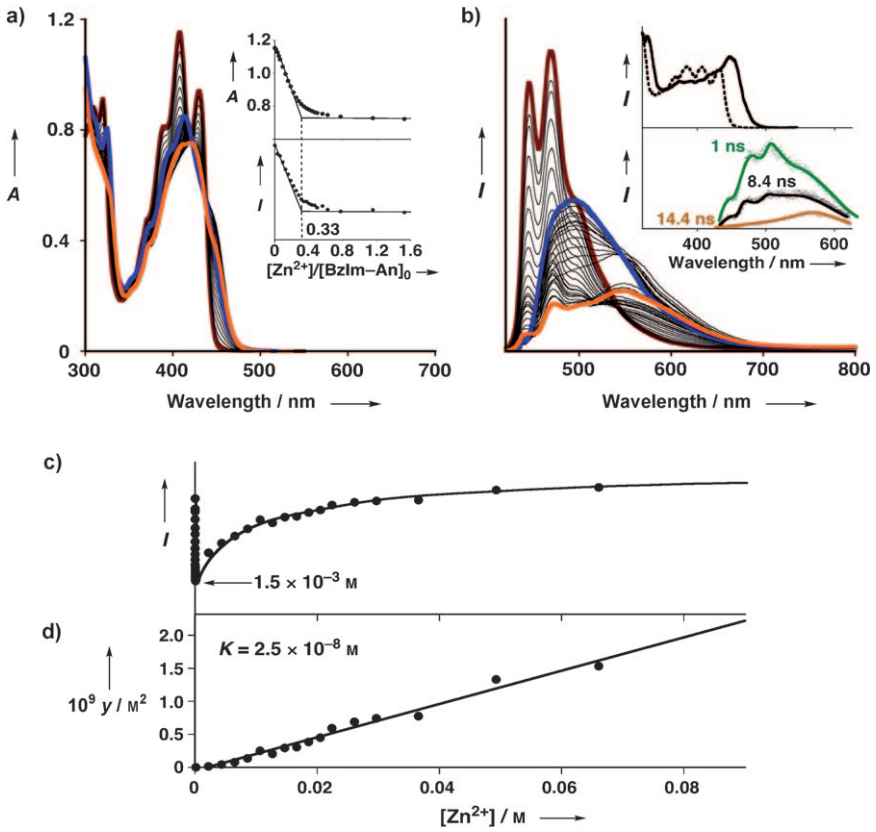

Figure 2. a) UV/Vis and b) fluorescence spectra of BzIm-An (5.0×10^{-5} M) in the presence of Zn^{2+} [0 M (red line) to 7.5×10^{-5} M (yellow line) to 6.6×10^{-2} M (blue line)] in MeCN at 298 K. Excitation wavelength $\lambda = 438$ nm. Plots of c) emission intensity at $\lambda = 494$ nm and d) $y = 0.75\,[\text{BzIm-An}]_0^2\,\alpha^3(1-\alpha)^{-1}$ versus $[Zn^{2+}]$ for the titration of BzIm-An (5.0×10^{-5} M) by Zn^{2+} in MeCN at 298 K. Insets: a) Plots of absorbance at $\lambda = 408$ (top) and emission intensity at $\lambda = 494$ nm (bottom) versus $[Zn^{2+}]/[\text{BzIm-An}]_0$. b) Excitation spectra of BzIm-An (5.0×10^{-5} M) in the presence of Zn^{2+} (6.0×10^{-4} M) recorded at $\lambda = 444$ (dashed line) and 554 nm (solid line) [top]. Time-resolved emission spectra of BzIm-An (5.0×10^{-5} M) in the presence of Zn^{2+} (6.0×10^{-4} M) monitored at 1.0, 8.4, and 14.4 ns (green, black, and dark yellow lines, respectively) after laser excitation at $\lambda = 400$ nm (bottom).

($> 1.5\times10^{-3}$ M) can be converted into a linear relation (Figure 2d) given by Equation (1), where $\alpha = (I-I_0)$-

$$K[Zn^{2+}] = 0.75\,[\text{BzIm-An}]_0^2\,\alpha^3(1-\alpha)^{-1} \quad (1)$$

$(I_\infty - I_0)^{-1}$, K is the equilibrium constant for conversion of $[\{(\text{BzIm-An})_3Zn^{2+}\}_2]$ into a 2:1 complex $[(\text{BzIm-An})_2Zn^{2+}]$, I_0 and I_∞ are emission intensities of $[\{(\text{BzIm-An})_3Zn^{2+}\}_2]$ and $[(\text{BzIm-An})_2Zn^{2+}]$ at $\lambda = 494$ nm, respectively [for derivation of Equation (1), see the Supporting Information S2]. Equation (1) is a fitting equation for a 2:1 model, and a good linear correlation in Figure 2d indicates that $[\{(\text{BzIm-An})_3Zn^{2+}\}_2]$ is converted into a simple 2:1 complex $[(\text{BzIm-An})_2Zn^{2+}]$ at the high-concentration region of Zn^{2+}.[20] The $[(\text{BzIm-An})_2Zn^{2+}]$ complex was detected by ESI MS (see the Supporting Information S4). K was determined to be 2.5×10^{-8} M from the slope of the linear plot of y versus $[Zn^{2+}]$ (Figure 2d). The small K value indicates that $[\{(\text{BzIm-An})_3Zn^{2+}\}_2]$ is thermodynamically favored over $[(\text{BzIm-An})_2Zn^{2+}]$, whereby $[\{(\text{BzIm-An})_3Zn^{2+}\}_2]$ is stabilized by multiple π-stacking interactions.

Such multiple π-stacking interactions in $[\{(\text{BzIm-An})_3Zn^{2+}\}_2]$ were confirmed by NOE experiments (see below). The ^{1}H and NOE NMR spectra of BzIm-An in the presence of Zn^{2+} are shown in Figure 3b–d.[21] Specifically, anthracene protons (H-*b*, H-*c*, H-*d*, and H-*e*) of $[\{(\text{BzIm-An})_3Zn^{2+}\}_2]$ (Figure 3b) show notable upfield shift relative to those of ligand BzIm-An (Figure 3a),[22] indicating the shielding effects from the neighboring aromatic rings (anthracene and benzimidazole moieties). NOE effects are observed between the H-*g* (or H-*f*) atom of the benzimidazole ring and the H-*c* atom of the anthracene ring (Figure 3c) as well as between the H-*a* atom and the H-*c* atom of the anthracene rings (Figure 3d), whereas there is no NOE between them for free BzIm-An (see the Supporting Information S5). These NOE effects clearly indicate π-stacking interactions between the anthracene and the benzimidazole rings as well as between the anthracene rings in $[\{(\text{BzIm-An})_3Zn^{2+}\}_2]$. To investigate possible π-stacking interactions in $[\{(\text{BzIm-An})_3Zn^{2+}\}_2]$, the structures of $[\{(\text{BzIm-An})_3Zn^{2+}\}_2]$ were modeled by the Merck Molecular Force Field (MMFF94)[23] (Figure 3e,f), where the vacant sites of $[\{(\text{BzIm-An})_3Zn^{2+}\}_2]$ are occupied by counter anions ($OSO_2CF_3^-$).[24] Two types of π-stacking interactions were found in the structure of $[\{(\text{BzIm-An})_3Zn^{2+}\}_2]$ (Figure 3f): π stacking between the anthracene and benzimidazole rings (dashed yellow lines) and between the anthracene rings (dashed red line). Thus, $[\{(\text{BzIm-An})_3Zn^{2+}\}_2]$ is stabilized by multiple π-stacking interactions between the anthracene chromophores and undergoes additional stabilization by donor/acceptor π-stacking interactions between anthracene and Zn^{2+}-coordinated benzimidazole rings.[25]

The π-stacking interactions between the anthracene and benzimidazole moieties were further confirmed by a synthesized reference compound, 2-(anthracen-9-ylethynyl)-1-methylimidazole (Im-An), where the 1-methylbenzimidazole ring of BzIm-An was replaced by a 1-methylimidazole ring to suppress π–π interactions with the anthracene units. Im-An also undergoes stepwise complex formation with Zn^{2+} to build two successive zinc complexes, $[\{(\text{Im-An})_3Zn^{2+}\}_2]$ and $[(\text{Im-An})_2Zn^{2+}]$ (Scheme 1b; see the Supporting Information S6). Both complexes were detected by ESI MS. The positive-ion ESI mass spectrum of a solution of Im-An and Zn^{2+} in MeCN shows isotopically resolved signals at *m*/*z* 2135.2 and 777.1 (Figure 3g,h), which correspond to $\{[Zn(\text{Im-An})_3]_2(OSO_2CF_3)_2(OH)\}^+$ and $\{[Zn(\text{Im-An})_2](OSO_2CF_3)\}^+$, respectively.[26–28] The characteristic distribu-

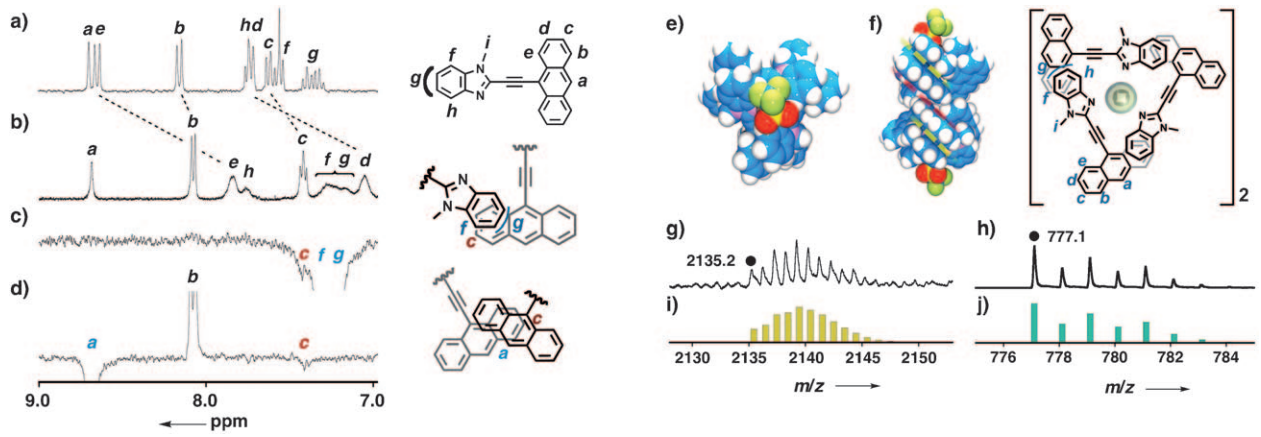

Figure 3. ^{1}H NMR (a,b) or NOE (c,d) spectra of BzIm-An (1.6×10^{-2} M) in the a) absence and b–d) presence of Zn^{2+} (1.3×10^{-2} M) in CD_3CN at 298 K. Without (b) or with irradiation of H-*g* (or H-*f*) (c) or H-*a* protons (d). e,f) Structures of $[\{(BzIm\text{-}An)_3Zn^{2+}\}_2]$ modeled by MMFF94: e) top view and f) front view. C blue; N purple; O red; S yellow; F dark yellow; H white. Red and yellow dashed lines denote the π stacking between the anthracene rings and that between anthracene and benzimidazole rings, respectively. g–j) Positive-ion ESI MS of a solution of Im-An (1.5×10^{-3} M) in MeCN in the presence of Zn^{2+} (1.5×10^{-3} M) with isotopically resolved signals and the calculated isotopic distributions for $\{[Zn(Im\text{-}An)_3]_2(OSO_2CF_3)_2(OH)\}^+$ and $\{[Zn(Im\text{-}An)_2](OSO_2CF_3)\}^+$.

tion of isotopomers in those signals agrees closely with their calculated isotopic distributions (Figure 3i,j). The equilibrium constant ($K=3.4\times10^{-7}$ M) for conversion of $[\{(Im\text{-}An)_3Zn^{2+}\}_2]$ into $[(Im\text{-}An)_2Zn^{2+}]$ is approximately 14 times larger than that for conversion of $[\{(BzIm\text{-}An)_3Zn^{2+}\}_2]$ into $[(BzIm\text{-}An)_2Zn^{2+}]$ ($K=2.5\times10^{-8}$ M) [see the Supporting Information S6]. The larger K value indicates that π-stacking interactions between anthracene and imidazole moieties in $[\{(Im\text{-}An)_3Zn^{2+}\}_2]$ are suppressed relative to those in $[\{(BzIm\text{-}An)_3Zn^{2+}\}_2]$, which induces a shift in the equilibrium in favor of the dissociation of $[\{(Im\text{-}An)_3Zn^{2+}\}_2]$ to $[(Im\text{-}An)_2Zn^{2+}]$ (rightward arrow in the second step of Scheme 1b) relative to the BzIm-An/Zn^{2+} system (Scheme 1a).

With these results in hand, we examined the emission selectivity of BzIm-An to Zn^{2+} over a wide range of competing metal ions. The emission response of BzIm-An to a series of metal ions is summarized in Figure 4 (for UV/Vis absorption and fluorescence spectra, see the Supporting Information S8). BzIm-An provides insignificant changes in emission color for competing metal ions, whereas it exhibits a visually noticeable blue-to-light-yellow emission color change upon addition of 5.0×10^{-4} M of Zn^{2+} (Figure 4a). The corresponding CIE chromaticity diagram shows the high selectivity of BzIm-An to Zn^{2+} (Figure 4b).[29,30]

In conclusion, we have achieved a highly selective ratiometric emission color change in BzIm-An by adjusting the concentration of Zn^{2+}. BzIm-An forms the 6:2 complex ($[\{(BzIm\text{-}An)_3Zn^{2+}\}_2]$) upon addition of Zn^{2+}, allowing a distinct color change in emission from blue to light yellow, whereas no appreciable change in emission color is observed for a wide range of competing metal ions. With increased concentrations of Zn^{2+}, the $[\{(BzIm\text{-}An)_3Zn^{2+}\}_2]$ complex is converted into a 2:1 complex $[(BzIm\text{-}An)_2Zn^{2+}]$, which exhibits green emission. The spectral signature of the anthracene dimer emission from $[\{(BzIm\text{-}An)_3Zn^{2+}\}_2]$ is sufficiently different from that of monomer fluorescence from free BzIm-An as well as that of $[(BzIm\text{-}An)_2Zn^{2+}]$. Thus, BzIm-An acts as a unique ligand that shows a continuous emission color change as a function of Zn^{2+} concentration, providing quantitative information about the amount of the target metal ion. This unique

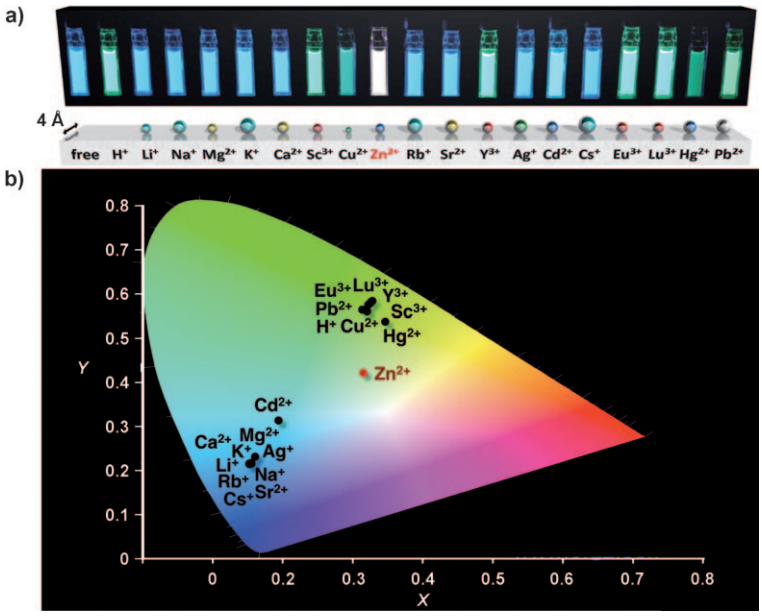

Figure 4. a) Visible fluorescence response of BzIm-An (5.0×10^{-5} M) in the presence of metal ions (5.0×10^{-4} M) and of trifluoroacetic acid (5.0×10^{-4} M) in MeCN at 298 K. ClO_4^- salts for Li^+, Na^+, Mg^{2+}, K^+, Ca^{2+}, Cu^{2+}, Rb^+, Sr^{2+}, Ag^+, Cd^{2+}, Cs^+, Hg^{2+}, and Pb^{2+}; $OSO_2CF_3^-$ salts for Sc^{3+}, Zn^{2+}, Y^{3+}, Eu^{3+}, and Lu^{3+}; effective ion radii for coordination number 8 shown. b) Fluorescence response shown on the CIE chromaticity diagram.

assembly strategy may open up new opportunities to create novel supramolecular systems and for use as sensing molecules.

Received: March 20, 2010
Published online: June 11, 2010

Keywords: arenes · dimerization · photochemistry · π interactions · self-assembly

[1] a) A. P. de Silva, H. Q. N. Gunaratne, T. Gunnlaugsson, A. J. M. Huxley, C. P. McCoy, J. T. Rademacher, T. E. Rice, *Chem. Rev.* **1997**, *97*, 1515; b) R. Y. Tsien in *Fluorescent Chemosensors for Ion and Molecule Recognition* (Ed.: A. W. Czarnik), American Chemical Society, Washington, DC, **1993** (ACS Symp. Ser. 538).

[2] a) K. Rurack, U. Resch-Genger, *Chem. Soc. Rev.* **2002**, *31*, 116; b) B. Valeur, I. Leray, *Coord. Chem. Rev.* **2000**, *205*, 3.

[3] a) E. L. Que, D. W. Domaille, C. J. Chang, *Chem. Rev.* **2008**, *108*, 1517; b) P. Jiang, Z. Guo, *Coord. Chem. Rev.* **2004**, *248*, 205; c) S. C. Burdette, S. J. Lippard, *Coord. Chem. Rev.* **2001**, *216*, 333; d) C. J. Chang, S. J. Lippard in *Neurodegenerative Diseases and Metal Ions, Vol. 1* (Eds.: A. Sigel, H. Sigel, R. K. O. Sigel), Wiley, Chichester, **2006**, pp. 321 – 370; e) E. Kimura, T. Koike, *Chem. Soc. Rev.* **1998**, *27*, 179; f) K. Kikuchi, K. Komatsu, T. Nagano, *Curr. Opin. Chem. Biol.* **2004**, *8*, 182.

[4] a) J.-M. Lehn, A. V. Eliseev, *Science* **2001**, *291*, 2331; b) S. J. Rowan, S. J. Cantrill, G. R. L. Cousins, J. K. M. Sanders, J. F. Stoddart, *Angew. Chem.* **2002**, *114*, 938; *Angew. Chem. Int. Ed.* **2002**, *41*, 898; c) S. Otto, R. L. E. Furlan, J. K. M. Sanders, *Science* **2002**, *297*, 590; d) P. T. Corbett, J. Leclaire, L. Vial, K. R. West, J.-L. Wietor, J. K. M. Sanders, S. Otto, *Chem. Rev.* **2006**, *106*, 3652; e) A. V. Davis, R. M. Yeh, K. N. Raymond, *Proc. Natl. Acad. Sci. USA* **2002**, *99*, 4793.

[5] a) R. S. K. Kishore, V. Kalsani, M. Schmittel, *Chem. Commun.* **2006**, 3690; b) K. Mahata, M. Schmittel, *J. Am. Chem. Soc.* **2009**, *131*, 16544.

[6] a) Y. Kubota, S. Sakamoto, K. Yamaguchi, M. Fujita, *Proc. Natl. Acad. Sci. USA* **2002**, *99*, 4854; b) S. Tashiro, M. Tominaga, T. Kusukawa, M. Kawano, S. Sakamoto, K. Yamaguchi, M. Fujita, *Angew. Chem.* **2003**, *115*, 3389; *Angew. Chem. Int. Ed.* **2003**, *42*, 3267.

[7] a) S. Hiraoka, T. Yi, M. Shiro, M. Shionoya, *J. Am. Chem. Soc.* **2002**, *124*, 14510; b) K. Harano, S. Hiraoka, M. Shionoya, *J. Am. Chem. Soc.* **2007**, *129*, 5300.

[8] T. Haino, T. Fujii, A. Watanabe, U. Takayanagi, *Proc. Natl. Acad. Sci. USA* **2009**, *106*, 10477.

[9] a) P. N. W. Baxter, *Chem. Eur. J.* **2002**, *8*, 5250; b) P. N. W. Baxter, *Chem. Eur. J.* **2003**, *9*, 2531.

[10] a) J. Yuasa, S. Fukuzumi, *J. Am. Chem. Soc.* **2006**, *128*, 15976; b) J. Yuasa, S. Fukuzumi, *J. Am. Chem. Soc.* **2008**, *130*, 566.

[11] S. Goswami, D. Sen, N. K. Das, *Org. Lett.* **2010**, *12*, 856.

[12] L. Zhang, R. J. Clark, L. Zhu, *Chem. Eur. J.* **2008**, *14*, 2894.

[13] a) J. N. Wilson, U. H. F. Bunz, *J. Am. Chem. Soc.* **2005**, *127*, 4124; b) A. J. Zucchero, J. N. Wilson, U. H. F. Bunz, *J. Am. Chem. Soc.* **2006**, *128*, 11872; c) S. M. Brombosz, A. J. Zucchero, R. L. Phillips, D. Vazquez, A. Wilson, U. H. F. Bunz, *Org. Lett.* **2007**, *9*, 4519.

[14] The ethyne spacer was introduced to provide diverse ligand conformations; see: a) M. Levitus, K. Schmieder, H. Ricks, K. D. Shimizu, U. H. F. Bunz, M. A. Garcia-Garibay, *J. Am. Chem. Soc.* **2001**, *123*, 4259; b) T. Terashima, T. Nakashima, T. Kawai, *Org. Lett.* **2007**, *9*, 4195; c) P. K. Sudeep, P. V. James, K. G. Thomas, P. V. Kamat, *J. Phys. Chem. A* **2006**, *110*, 5642; d) M. Levitus, M. A. Garcia-Garibay, *J. Phys. Chem. A* **2000**, *104*, 8632; e) J. M. Seminario, A. G. Zacarias, J. M. Tour, *J. Am. Chem. Soc.* **1998**, *120*, 3970.

[15] Multicomponent supramolecular probes that bring the two chromophores in a face-to-face arrangement upon binding metal ions have been restricted to stoichiometries of 2:1 to 3:1; see: a) R.-H. Yang, W.-H. Chan, A. W. M. Lee, P.-F. Xia, H.-K. Zhang, K. A. Li, *J. Am. Chem. Soc.* **2003**, *125*, 2884; b) M. Licchelli, L. Linati, A. O. Biroli, E. Perani, A. Poggi, D. Sacchi, *Chem. Eur. J.* **2002**, *8*, 5161; c) B. Bodenant, F. Fages, M.-H. Delville, *J. Am. Chem. Soc.* **1998**, *120*, 7511; d) H. J. Kim, J. Hong, A. Hong, S. Ham, J. H. Lee, J. S. Kim, *Org. Lett.* **2008**, *10*, 1963.

[16] a) S. Welsch, B. Nohra, E. V. Peresypkina, C. Lescop, M. Scheer, R. Réau, *Chem. Eur. J.* **2009**, *15*, 4685; b) A. Kishimura, T. Yamashita, T. Aida, *J. Am. Chem. Soc.* **2005**, *127*, 179; c) H. Maeda, Y. Haketa, T. Nakanishi, *J. Am. Chem. Soc.* **2007**, *129*, 13661.

[17] a) B. L. Vallee, K. H. Falchuk, *Physiol. Rev.* **1993**, *73*, 79; b) C. J. Frederickson, J.-Y. Koh, A. I. Bush, *Nat. Rev. Neurosci.* **2005**, *6*, 449.

[18] a) E. Berni, C. Dolain, B. Kauffmann, J.-M. Léger, C. Zhan, I. Huc, *J. Org. Chem.* **2008**, *73*, 2687; b) Y. Molard, D. M. Bassani, J.-P. Desvergne, N. Moran, J. H. R. Tucker, *J. Org. Chem.* **2006**, *71*, 8523; c) P. P. Neelakandan, D. Ramaiah, *Angew. Chem.* **2008**, *120*, 8535; *Angew. Chem. Int. Ed.* **2008**, *47*, 8407.

[19] The emission quantum yield of BzIm-An [(92 ± 2) %] decreased to 44 % in the [{(BzIm-An)$_3$Zn^{2+}}$_2$] complex.

[20] It should be noted that fitting of the saturated dependence of the emission intensity (Figure 2c) failed with a 1:1 model (see the Supporting Information S3).

[21] The ^{1}H NMR spectrum of BzIm-An in the presence of a large excess of Zn^{2+} could not be examined because $Zn(OTf)_2$ was not soluble in CD_3CN at high concentrations.

[22] The ^{1}H NMR spectrum of [{(BzIm-An)$_3$Zn^{2+}}$_2$] with symmetrical patterns indicates medium exchange between free and complexed BzIm-An.

[23] a) T. A. Halgren, *J. Comput. Chem.* **1996**, *17*, 490; b) T. A. Halgren, *J. Comput. Chem.* **1996**, *17*, 520.

[24] For a Zn^{2+} complex with imidazole derivatives in a tetrahedral geometry, see: Y.-H. Xu, Y.-Q. Lan, Y.-H. Zhao, D.-Y. Du, G.-J. Xu, K.-Z. Shao, Z.-M. Su, Y. Liao, *Inorg. Chem. Commun.* **2009**, *12*, 169.

[25] The [{(BzIm-An)$_3$Zn^{2+}}$_2$] complex was dispersed in a toluene solution, which interfered with π-stacking interactions in [{(BzIm-An)$_3$Zn^{2+}}$_2$] (see the Supporting Information S7).

[26] A counteranion of [{(Im-An)$_3$Zn^{2+}}$_2$] is replaced by OH^- in the ionization process. OH^- may come from water contained in MeCN.

[27] The [{(BzIm-An)$_3$Zn^{2+}}$_2$] complex could not be detected, whereas [{(Im-An)$_3$Zn^{2+}}$_2$] was detected by ESI MS, indicating that the benzimidazole unit affects the ionization process somewhat.

[28] Both [(BzIm-An)$_2$Zn^{2+}] and [{(BzIm-An)$_3$Zn^{2+}}$_2$] can be detected by ESI MS when these complexes interconvert in equilibrium.

[29] The emission of BzIm-An in the presence of Zn^{2+} is not influenced by competing metal ions (see the Supporting Information S7).

[30] BzIm-An also shows light yellow emission due to anthracene dimer in the presence of a high concentration of Zn^{2+} (5.0×10^{-2} M) in water, when conversion into [(BzIm-An)$_2$Zn^{2+}] is retarded by the presence of water (see the Supporting Information S7).

